Analogue Receiver for Coherent Optical Analogue Radio-over-Fiber Transmission

BERNHARD SCHRENK,[1,*] MARKUS HOFER,[1] THOMAS ZEMEN[1]

[1] *AIT Austrian Institute of Technology, Dept. Digital Safety&Security / Security & Communication Technologies, Vienna 1220, Austria.*
**Corresponding author: bernhard.schrenk@ait.ac.at*

Received 06 June 2017; revised 19 July, 2017; accepted XX Month XXXX; posted XX Month XXXX (Doc. ID XXXXX); published XX Month XXXX

A receiver for low-cost coherent optical applications is presented. Conceptual simplicity is guaranteed through use of a monolithic integrated externally modulated laser. Local oscillator and fast photodetector are provided by the distributed feedback section and electro-absorption modulator of the monolithic laser. The injection locking feature, which is obtained in virtue of the in-line configuration of the receiver, guarantees exact frequency translation during coherent reception and obviates the need for digital signal processing typically employed for the purpose of signal recovery. The proposed receiver is experimentally demonstrated for wired multi-carrier and analogue transmission of wireless radio signals. Nyquist-shaped frequency division multiplexing with data rates of up to 10 Gb/s and real-time transmission of 64-ary quadrature amplitude modulated narrowband orthogonal frequency division multiplexed radio signals is shown for an optical loss budget of 31 dB.

OCIS codes: *(060.1660) Coherent communications; (140.3520) Lasers, injection-locked; (230.5160) Photodetectors; (060.5625) Radio frequency photonics; (060.2360) Fiber optics links and subsystems.*

http://dx.doi.org/00.0000/OL.99.099999

Continuous progress in digital data transmission has enabled telecom and datacom networks to keep pace with vigorously growing data traffic volumes. Photonic technology prevails over electronic legacy systems as data rates and channel capacity increases. Nonetheless, digital signal processing (DSP) takes a more and more important role in opto-electronic front-ends once highly complex signals are adopted [1]. Lean solutions based on analogue photonics and analogue electrical signal conditioning are considered an attractive alternative due to their conceptual simplicity that goes along with cost- and energy efficiency. Especially in combination with optical fronthauling of radio signals [2], the ongoing network densification and surging mobile data rates, analogue receivers are expected to play an important role in near future. However, the performance requirements in terms of linearity while further offering broadband operation are demanding. At the same time the increasing prevalence of coherent optical data communication is propelling metro-core networks and suggests such detection concepts even for the last mile as commodity optics based on direct detection is slowly reaching its limits in terms of guaranteed bandwidth and optical spectral efficiency.

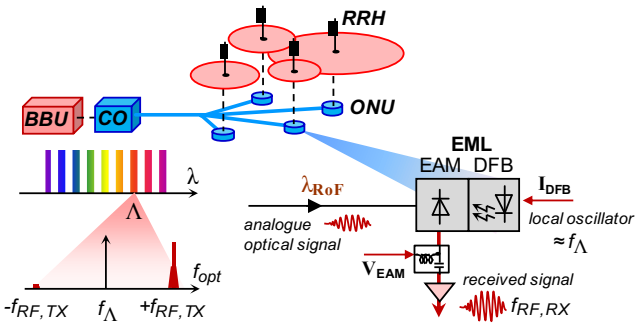

Fig. 1. Coherent EML-based receiver for analogue optical radio-over-fiber transmission without auxiliary optical DSP functions.

In this letter we propose a simple analogue coherent optical reception scheme with injection locking for its local oscillator and DSP-less retention of signal integrity. We exploit an externally modulated laser (EML) not as transmitter but as monolithic integrated coherent optical detector and experimentally demonstrate reception of a four-channel Nyquist-shaped frequency division multiplexed (FDM) quadrature amplitude modulated (QAM) signal at 1 Gbaud symbol rate per sub-channel. We further validate coherent reception of a 64-QAM orthogonal FDM (OFDM) analogue radio-over-fiber signal without the need for additional offset correction for its carrier frequency.

The proposed coherent optical reception scheme is fueled by the absorption and light generation capabilities of an EML (Fig. 1). The electro-absorption modulator (EAM) section is known for high-bandwidth modulation with high efficiency. As has been proven previously, its absorption feature does further allow for opto-electronic signal conversion [3, 4]. The provision of a high-bandwidth photodetector together with a monolithically

integrated distributed feedback (DFB) light source enables the EML to serve as coherent detector within the spectral range covered by its DFB-based local oscillator. Such a scheme has been recently exploited for the purpose of photonic up-conversion [5]. Moreover, coherent multiplexing schemes where a particular target channel at Λ is selected among multiple transmitted channels are feasible since temperature and DFB current I_{DFB} can be adjusted to lock the DFB emission wavelength on Λ. Figure 1 sketches a potential application scenario in combination with analogue radio-over-fiber transmission. Different signals are generated at the baseband unit (BBU) and broadcasted by the central office (CO) to multiple optical network units (ONU). The ONUs select one of the narrowly-spaced wavelength channels and converts it to the radio frequency (RF) domain to feed the remote radio head (RRH) at the antenna site. In case of analogue radio-over-fiber transmission the radio signal is transmitted at its carrier frequency $f_{RF,TX}$ on the optical carrier frequency f_Λ so that no energy-hungry and costly digitization is required at the opto-electronic front-ends. Especially for high-data rate mm-wave signals such as endeavored for the future 5G radio standard, this can guarantee a high degree of sub-system simplicity for the network terminals. In case of coherent reception, however, the spectral alignment of the local oscillator at the ONU with the target channel wavelength Λ at the CO is challenging if no further DSP is to be employed for the purpose of frequency offset compensation or other signal recovery purposes. Here the EML-based coherent receiver with its in-line EAM photodetector can be beneficial as it enables fine locking of its DFB emission to the incident optical carrier frequency f_Λ, as we will prove shortly. Thanks to this wavelength locking property the received radio carrier frequency $f_{RF,RX}$ perfectly resembles its transmitted counter-part $f_{RF,TX}$, as it would be the case in direct-detection schemes. The injection locking feature of the EML therefore obviates complex optical DSP functions at the receiver, thus yielding high conceptual simplicity. At the same time the sensitivity and multiplexing gain of coherent reception can be exploited and enables a high loss budget and high spectral occupancy for the optical distribution network as known for ultra-dense wavelength division multiplexing [6].

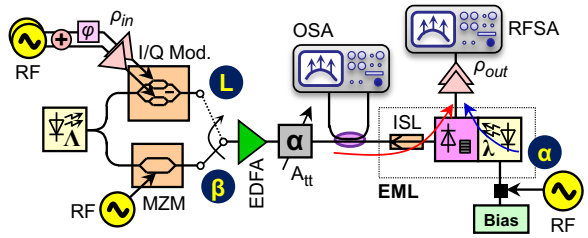

Fig. 2. Experimental setup for acquiring key characteristics of the EML for its use as coherent detector.

In order to prove the concept a commercial EML device (NEL NLK3C8) intended for operation at the ITU-T channel C47 was first characterized and then employed in a representative evaluation scenario. The setup for device characterization is presented in Fig. 2. The butterfly-packaged EML did include a hybridly integrated optical isolator (ISL), which apparently prohibits the injection of signals into the EML receiver. However, its high reverse transmission loss governed by its isolation property can still be overcome in virtue of the sensitivity gain experienced through coherent optical detection. The isolation will be therefore de-embedded from the receiver for loss budget calculations to associate it with external losses during applicability studies. It is characterized together with absorption and injection locking.

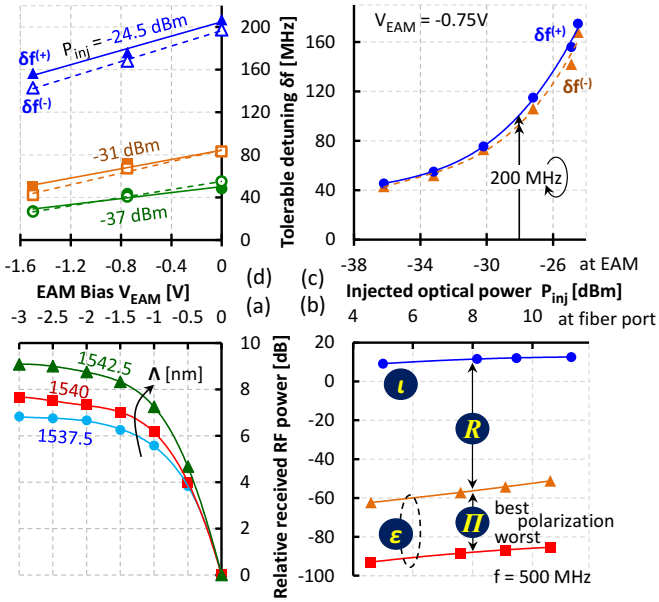

Fig. 3. EML characteristics. (a) Opto-electronic absorption of the EAM, (b) isolation loss and polarization dependent response, and injection locking range as function of (c) optical input power and (d) EAM bias.

Figure 3(a) shows the relative opto-electronic absorption of the EML as function of the reverse EAM bias and referenced to the unbiased EAM at V_{EAM} = 0V. The absorption relates to the responsivity of the EAM as photodetector. A tone at 500 MHz modulated on an optical wavelength Λ was injected into the EML and the converted electrical signal was monitored with a RF spectrum analyzer (RFSA). The DFB section of the EML was left unbiased at this point. The absorption features a steep slope at low EAM bias and reaches a magnitude of 5.6 to 7.3 dB relative to the unbiased EAM for a bias of -1V. Although Fig. 3(a) may suggest that the EAM is more efficient for longer wavelengths, this results from the fact that the red-shift of the absorption edge when applying a reverse bias leads to a larger change in relative absorption; However, when looking at the absolute absorption magnitude for V_{EAM} = 0V, there is an 8 dB penalty for the signal at 1542.5 nm (▲) when compared to 1540 nm (■), while the shorter wavelength at 1537.5 nm (●) benefits by a 2.5 dB increased sensitivity.

The reverse transmission loss of the integrated isolator has been characterized by sequentially comparing the detected magnitudes of the external signal Λ (β in Fig. 2) with that of a tone modulated on the biased DFB section (α). By monitoring the optical injection levels through an optical spectrum analyzer (OSA) at the fiber port of the EML, the detected magnitudes of the tones can be related and deviate by the loss the isolator is introducing to the external signal. Figure 3(b) shows the detected power level for external (*ε*) and DFB (*ι*) injection. For the external signal the absorption strongly depends on the incident state of polarization. The detected magnitude drops in case the worst state (■) is launched, according to a polarization dependent response of -15.1 dB (*Π*).

For the DFB signal (●) co-polarization with the preferred axis of the EAM detector is ensured through the monolithic integrated design. Comparing the response of the respective external (▲) and the DFB signal, an isolation of 33.9 dB (*R*) has been found. It shall be stressed that coherent reception as performed later in this letter will require co-polarization between the injected data signal and the local oscillator provided by the DFB, or, alternatively, polarization management strategies such as diversity reception.

An important characteristic to practically exploit wavelength locking is the tolerable frequency detuning Δf for which stable locking between the externally injected signal at Λ and DFB emission can be obtained. This range has been measured by observation of the beat note for the detected EAM signal in terms of a positive ($\delta f^{(+)}$) and negative ($\delta f^{(-)}$) detuning at which the DFB is still pulled to Λ. The power of the injected signal (β) has been further varied through a variable attenuator (A_{tt}). Figure 3(c) shows these detunings for a fixed EAM bias of V_{EAM} = -0.75V as function of the injected power level. The locking range $\Delta f = \delta f^{(+)} + \delta f^{(-)}$ reaches 200 MHz for an injected power of -27.8 dBm and decreases as the injected signal weakens. However, the obtained range is still much larger than typical wavelength drifts of thermo-electrically stabilized EML devices so that stable locking can be obtained. Since the magnitude of injected light into the DFB section strongly depends on the actual absorption at the EAM section, Fig. 3(d) presents the locking ranges for various EAM bias points V_{EAM}. The compatible frequency detuning decreases to ~50 MHz for an input of -31 dBm and a higher reverse EAM bias of -1.5V, in good agreement with Figs. 3(c) and 3(a). DFB wavelength tuning for initial locking can be done through control of bias current and temperature with efficiencies of 0.87 GHz/mA at a DFB bias of 115 mA and 13.4 GHz/°C, respectively.

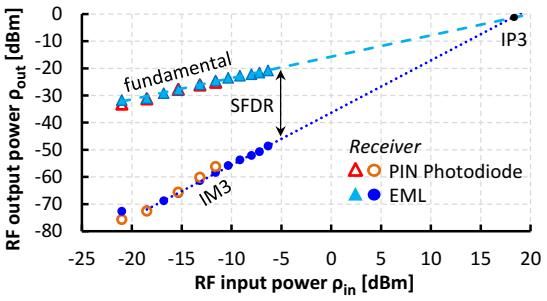

Fig. 4. End-to-end inter-modulation distortion for the photonic link.

The linearity of the end-to-end coherent radio transmission link (ρ_{in} to ρ_{out} in Fig. 2) was evaluated through third-order inter-modulation (IM3) measurements, for which two tones at 1 GHz +/- 5 MHz have been optically single-sideband modulated on the seed wavelength Λ through an optical I/Q modulator (L). Figure 4 presents the spurious-free dynamic range (SFDR) for the injection-locked EML-based coherent receiver (▲,●), which is compared to direct detection facilitated through a PIN photodiode (Δ,○). There is no degradation when using the EML-based receiver, which features a SFDR of 32.2 dB for a RF input power ρ_{in} of -10 dBm. The input-referred third-order interception point (IP3) for the analogue coherent photonic link is 18.2 dBm.

The proposed receiver based on the EML was subsequently evaluated for one-way wired multi-channel and analogue radio-over-fiber transmission. Two transmission formats have been chosen for evaluation. The first resembles a wired access scenario through a 4-channel broadband Nyquist-FDM signal with a symbol rate of 1 Gbaud per adaptively modulated sub-channel, having a roll-off factor of 0.5 and a channel spacing of 1.3 GHz. The second format addresses radio-over-fiber transmission through a narrowband OFDM signal comprising of 64 sub-carriers over a 20 MHz bandwidth, modulated by 16- or 64-ary QAM. The OFDM signal is up-converted to a carrier frequency of 5.7 GHz.

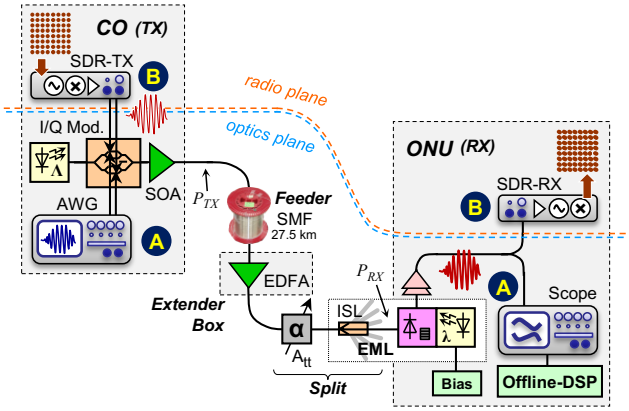

Fig. 5. Experimental setup for evaluating the EML-based receiver for coherent optical wired and analogue radio-over-fiber links.

The experimental setup that resembles such an access scenario is presented in Fig. 5. At the CO the optical transmitter performs optical single-sideband modulation of the data signal at the wavelength channel Λ = 1538.7 nm through an inphase-quadrature (I/Q) modulator. Data generation is facilitated through an arbitrary waveform generator (AWG) in case of the broadband Nyquist-FDM signal (A) and through the NI USRP-2953R software-defined radio (SDR) for the narrowband OFDM (B). The optical signal is then boosted by a semiconductor optical amplifier (SOA) and launched with a power level P_{TX} of 6 dBm.

The optical distribution network consists of a 27.5 km standard single-mode feeder fiber (SMF) and a concentrated loss emulating a passive splitter for distribution of the signal to multiple network terminals. This loss element is composed by a variable optical attenuator (A_{tt}) for conducting bit (BER) and block error ratio (BLER) measurements and the reverse isolation loss of 33.9 dB for the co-packaged EML isolator, which would not be present in a realistic deployment scenario but cannot be excluded from the EML device for this present investigation. As it is typical for modern access architectures with high concentrated loss towards the drop segment [7], an extender box based on an Erbium-doped fiber amplifier (EDFA) was included between feeder and split.

The receiver at the ONU is based on the foregoing EML-based coherent reception concept. For this the DFB section of the EML was tuned to the incident data signal at Λ through monitoring of the detected signal. Coarse tuning is performed by means of temperature control while fine adjustment to obtain injection locking is done by DFB bias current adjustment. The chosen EAM bias was -0.75V. The detected signal is pre-amplified and received by (A) a real-time oscilloscope for sub-sequent off-line DSP in case of the wired broadband Nyquist-FDM signal or by (B) a SDR receiver for real-time processing of the narrowband OFDM radio signal. In this latter radio-over-fiber case there has been no DSP

employed at the optical layer.

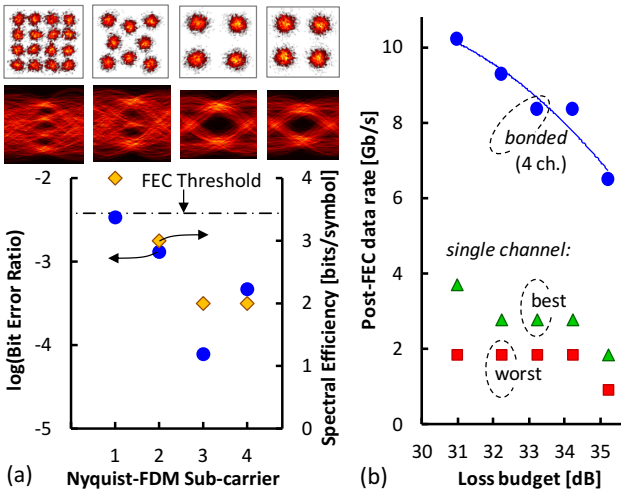

Fig. 6. (a) BER and spectral efficiency for a 4-channel Nyquist-FDM QAM shown at a received power level of -25 dBm. (b) Bonded Nyquist-FDM data rate as function of the optical loss budget.

The BER performance for all four subcarriers of the Nyquist FDM is shown in Fig. 6(a) for a received power P_{RX} of -25 dBm at the EAM input (see Fig. 5). A spectral efficiency (♦) of up to 4 bits/symbol can be supported for obtaining a BER (●) below the hard-decision forward error correction (FEC) threshold of 3.8×10^{-3}. The obtained QAM constellations and Nyquist-shaped eye diagrams validate that the spectrally flat broadband response of the EAM allows for high Gbaud symbol rates per sub-channel. The given bit loading leads to a per-channel data rate of up to 3.7 Gb/s in case of 16-QAM after accommodating the typical 7% FEC overhead. The aggregated data rate when bonding all four channels is 10.2 Gb/s. Figure 6(b) presents the dependency of the obtained data rate on the loss budget. As the spectral efficiency drops the capacity decreases at -0.87 Gb/s/dB (●). End-users with differing bandwidth demands can be allocated to best (▲) and worst (■) FDM channels. This allows to share the same transmission wavelength Λ by multiple ONUs to further improve the spectral occupancy. Note that the polarization state of the received signal was aligned with the EAM axis in order to yield its maximum response. In a realistic scenario, a diversity scheme would need to be adopted for polarization management.

Figure 7 presents the end-to-end BLER performance for the narrowband OFDM format as function of the optical loss budget between CO and ONU. Wavelength locking of the EML to the incident optical carrier Λ ensures that the radio carrier frequency of 5.7 GHz is exactly preserved even without DSP functions at the optical layer. This is evidenced by the clean 16- and 64-QAM constellation diagrams obtained after OFDM demodulation at the radio plane, which was conducted without addressing potential optical layer impairments. The error vector magnitude (EVM) for the presented 16- and 64-QAM constellations are 6.3 and 5.9%, respectively, and are therefore fulfilling the 3GPP requirements. The good transmission quality is further underpinned by BLER measurements, for which a payload size of 9024 bits/packet and different convolutional code rates R were used. In case of a 54 Mb/s 64-QAM OFDM with code rate R = 3/4 (♦) a reception sensitivity of -25.4 dBm is obtained at the BLER level of 10^{-2}. This corresponds to a compatible loss budget of 31.4 dB. For a more robust code rate of R = 2/3 (■) the 10^{-4} BLER level is obtained, which corresponds to the lowest BLER accessible for the given packet length used for real-time processing. This confirms that analogue transmission of the 64-QAM OFDM does not suffer from error floors despite the use of analogue coherent optical reception with the EML-based low-cost transmitter. For the 16-QAM OFDM high loss budgets of 40.6 and 44.1 dB are obtained for code rates R = 3/4 (▲) and R = 1/2 (●), respectively.

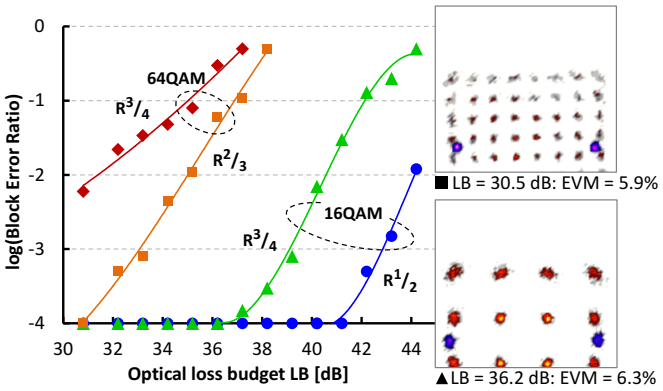

Fig. 7. BLER for analogue radio-over-fiber transmission of a 16/64-QAM OFDM as function of the optical loss budget.

It shall be stressed that in case of an unbiased DFB section at the EML receiver, which corresponds to the scenario of performing direct rather than coherent detection, the signal spectrum could not be recognized above the noise floor after opto-electronic signal conversion, neither for Nyquist-FDM nor for OFDM transmission.

The presented transmission performance for wired and wireless signals with an EML-based coherent receiver offering optical injection locking and thus obviating the need for optical DSP functions proves a simple signal detection concept for coherent analogue radio-over-fiber transmission. Bidirectional optical transmission in time division duplex or full-duplex mode is thinkable in virtue of the modulation capability of the EML.

Funding. Austrian Research Promotion Agency (FFG) (TRITON 858697)

References

1. X. Liu, H. Zeng, N. Chand, and F. Effenberger, J. Lightw. Technol. **34**, 1556 (2016).
2. C. Lim, A. Nirmalathas, M. Bakaul, P. Gamage, K.L. Lee, Y. Yang, D. Novak, and R. Waterhouse, J. Lightw. Technol. **28**, 390 (2010).
3. N.H. Zhu, H.G. Zhang, J.W. Man, H.L. Zhu, J.H. Ke, Y. Liu, X. Wang, H.Q. Yuan, L. Xie, and W. Wang, Opt. Expr. **17**, 22114 (2009).
4. M.P. Thakur, T.J. Quinlan, C. Bock, S.D. Walker, M. Toycan, S. Dudley, D.W. Smith, A. Borghesani, D. Moodie, M. Ran, and Y. Ben-Ezra, J. Lightw. Technol. **27**, 266 (2009).
5. M. Zhu, L. Zhang, S.H. Fan, C. Su, G. Gu, and G.K. Chang, Phot. Technol. Lett. **24**, 1127 (2012).
6. H.K. Shim, H. Kim, and Y.C. Chung, Opt. Expr. **22**, 29037 (2014).
7. M. Fujiwara, T. Imai, K. Taguchi, K.I. Suzuki, H. Ishii, and N. Yoshimoto, J. Lightw. Technol. **31**, 634 (2013).

Full References

1. X. Liu, H. Zeng, N. Chand, and F. Effenberger, "Efficient Mobile Fronthaul via DSP-Based Channel Aggregation," J. Lightwave Technol., Vol. 34, no. 6, pp. 1556-1564 (2016).
2. C. Lim, A. Nirmalathas, M. Bakaul, P. Gamage, K.L. Lee, Y. Yang, D. Novak, and R. Waterhouse, "Fiber-Wireless Networks and Subsystem Technologies," J. Lightwave Technol., Vol. 28, no. 4, pp. 390-405 (2010).
3. N.H. Zhu, H.G. Zhang, J.W. Man, H.L. Zhu, J.H. Ke, Y. Liu, X. Wang, H.Q. Yuan, L. Xie, and W. Wang, "Microwave generation in an electro-absorption modulator integrated with a DFB laser subject to optical injection", Opt. Expr., Vol. 17, no. 24, pp. 22114-22123 (2009).
4. M.P. Thakur, T.J. Quinlan, C. Bock, S.D. Walker, M. Toycan, S. Dudley, D.W. Smith, A. Borghesani, D. Moodie, M. Ran, and Y. Ben-Ezra, "480-Mbps, Bi-Directional, Ultra-Wideband Radio-Over-Fiber Transmission Using a 1308/1564-nm Reflective Electro-Absorption Transducer and Commercially Available VCSELs," J. Lightwave Technol., Vol. 27, no. 3, pp. 266-272 (2009).
5. M. Zhu, L. Zhang, S.H. Fan, C. Su, G. Gu, and G.K. Chang, "Efficient Delivery of Integrated Wired and Wireless Services in UDWDM-RoF-PON Coherent Access Network," Phot. Technol. Lett., Vol. 24, no. 13, pp. 1127-1129 (2012).
6. H.K. Shim, H. Kim, and Y.C. Chung, "Practical 12.5-Gb/s, 12.5-GHz spaced ultra-dense WDM PON," Opt. Expr., Vol. 22, no. 23, pp. 29037-29047 (2014).
7. M. Fujiwara, T. Imai, K. Taguchi, K.I. Suzuki, H. Ishii, and N. Yoshimoto, "Field Trial of 100-km Reach Symmetric-Rate 10G-EPON System Using Automatic Level Controlled Burst-Mode SOAs," J. Lightwave Technol., Vol. 31, no. 4, pp. 634-640 (2013).